

Lightweight design of vehicle structure with tailor rolled blank under crashworthiness

Libin Duan, Guangyong Sun, Junjia Cui, Tao Chen, Guangyao Li¹

State Key Laboratory of Advanced Design and Manufacturing for Vehicle Body,
Hunan University, Changsha, 410082, China, duanlibin_hnu@163.com

Abstract

Unlike existing uniform thickness structures, tailor rolled blank (TRB) which allows continuous metal thickness changes has been recently gaining comprehensive attention due to its excellent lightweight potential. The aim of this study is to combine the advantages of the TRB manufacturing technology with the structural optimization methodology to design the front longitudinal beam under impact load. First, a simplified frontal impact FE model was extracted from the full vehicle finite element model and experimentally verified. Then, the conventional uniform thickness inner panel was replaced with the TRB. Finally, the ε -SVR surrogate with artificial bee colony (ABC) algorithm was used to obtain the optimal thickness distribution of TRB. The results show that weight of TRB front longitudinal beam was reduced by 16.10%, while the crashworthiness was significantly improved.

Keywords: Tailor rolled blank (TRB); Front longitudinal beam (FLB); Crashworthiness optimization; Lightweight design

Introduction

Lightweight and crashworthiness design have being two challenges for automotive industry due to more and more strict safety regulations and environmental pressures. The conventional uniform thickness structures mainly use single material and uniform wall thickness. In fact, automotive components often bear very complex loading, implying that different regions should have different roles to maximize usage of materials. Obviously, potential of crashworthiness and lightweight of the conventional uniform thickness structures has not been fully exploited. In order to address the issue, some advanced manufacturing processes, such as tailor welded blank (TWB) and tailor rolled blank (TRB) have been presented and widely applied in automotive industry. For example, the inner door panel ^[1], B-pillar ^[2] and frontal side rail ^[3] are some typical examples for TWB structures adopted in vehicles. Compared with TWB, TRB varies the blank thickness with a continuous thickness transition, which leads to have better formability and greater weight reduction ^[4]. Due to the advantage of TRB, some researchers do some investigation to promote the application of TRB in vehicle industry. In this regards, Jeon et al. ^[5] developed a vehicle door inner panel using TRB. Sun and co-authors ^[6-7] studied the crashworthiness of TRB thin-walled structures under axial impact, and further compared comparatively the energy absorption characteristic between TRB columns and tapered tubes withstanding oblique impact load. Lately, Sun et al. ^[8] investigated the crashworthiness of TRB tubes under dynamic bending load. Though the TRB structures have excellent crashworthiness, it is by no mean easy to obtain the optimal thickness distribution. As an effective alternative, the structural optimization methodology is used to design the TRB parts. For example, Chuang et al. ^[9] adopted a multidisciplinary design optimization methodology to optimize the underbody parts considering multiple impact modes, seatbelt pull analysis and NVH.

It is well known that front longitudinal beam (FLB) is the most significant deformable part under vehicle frontal impact and its deformation pattern can greatly influence the vehicle safety ^[10]. To be authors' best knowledge, there have been very limited reports available on the crashworthiness design of front longitudinal beam with TRB (FLB-TRB). Therefore, the paper aims to performing the lightweight design of the FLB-TRB under crashworthiness criteria.

1. Frontal impact modeling and experimental verification

1.1 Proposed simplified frontal impact model

A single run of crashworthiness simulation for a full-scale vehicle often needs to spend more than 10 hours on some powerful computers ^[11]. Design optimization is an iterative process, which needs a lot of runs. Obviously, it is impractical to conduct design optimization using a finite element model of full-scale vehicle. Consequently, it is critical to construct an equivalent simplified FEM to largely reduce the expensively computational burden. Figure 1 shows these parts whose energy absorption (EA) ratios are large than 1% under 100% frontal impact.

¹ Corresponding Author: Telephone: +86-731-8882 1445; Email: gyli@hnu.edu.cn.

From which, it is easily found that the EA of FLB is more than half of energy dissipation of full-scale vehicle. From the perspective, the FLB is the most significant part under frontal impact. The other components such as roof, B-pillar, C-pillar, doors, rear frame, windscreen etc. have little effect on the crashworthiness, so these parts can be neglected to improve the computational efficiency. As we all known, the load transfer path has a significant effect on the deformation model and crashworthiness of parts. In order to maintain the original load transfer path after removing many unimportant parts, some equivalent square columns are added in the simplified frontal impact model. The full-scale vehicle and the corresponding simplified frontal impact model are impacted on a rigid wall with an initial velocity of 50 km/h, shown as in Figure 2.

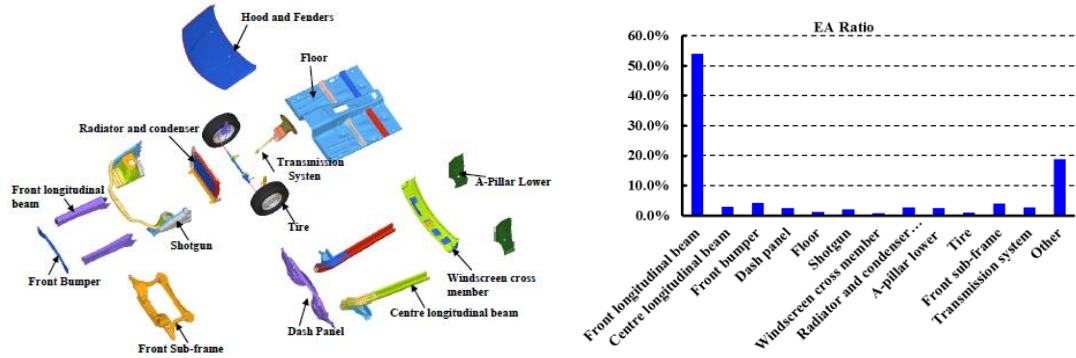


Figure 1: EA Ratio of key parts under frontal impact



Figure 2: Physical model and FE model under 100% frontal impact: (a) full-scale vehicle; (b) simplified frontal impact model

1.2 Experimental verification of numerical model

To conveniently describe the dynamic responses of the simulation and physical test, the following criteria are used: (1) the structural deformation; (2) the acceleration vs. time curve; and (3) the peak value and its corresponding time point. Figure 3 compares the structural deformations between the simulation and corresponding physical tests at t=120ms. The simulation results are agreed well with the results of physical tests regardless of the full-scale vehicle or the simplified frontal impact model. The deformation models of simulation and test for FLB are given in Figure 4. Figure 5 plots the deceleration histories of the numerical simulation and physical test at the left rocker of B-pillar. The pulses were filtered with CFC 60 Hz according to the standard of Society of Automotive Engineers (SAE) J211. It shows that the numerical simulations regardless of the full-scale vehicle or the simplified frontal impact model can very well capture the responses of test including the peak accelerations and the corresponding times. In addition, the results of the simplified frontal impact model are agreement with that of full-scale vehicle. According to the aforementioned analysis, the simplified frontal impact FEM can replace the full-scale vehicle FEM effectively to perform the subsequent design optimization.

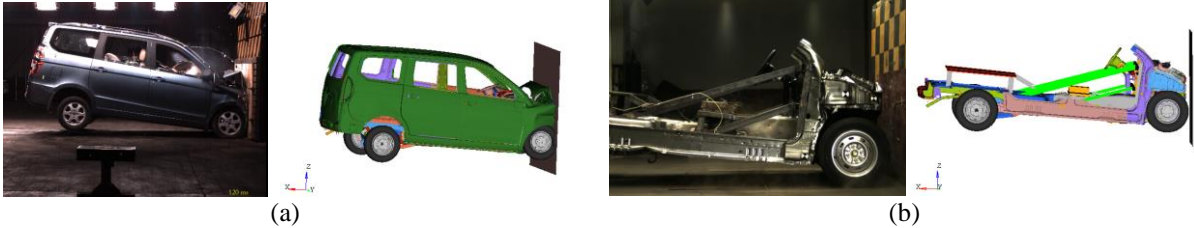


Figure 3: Comparison of deformation patterns between tests and numerical simulations at t=120 mm: (a) full-scale vehicle, (b) simplified frontal impact model.

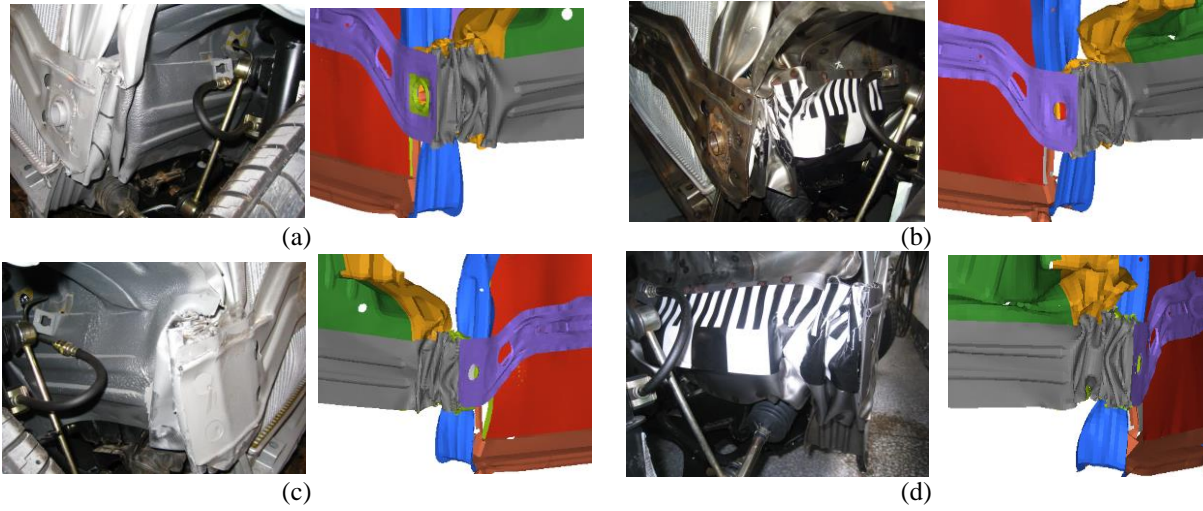


Figure 4: Comparison of FLB deformation patterns: (a) Left FLB of full-scale vehicle; (b) Left FLB of simplified frontal impact model; (c) Right FLB of full-scale vehicle; and (d) Right FLB of simplified frontal impact model

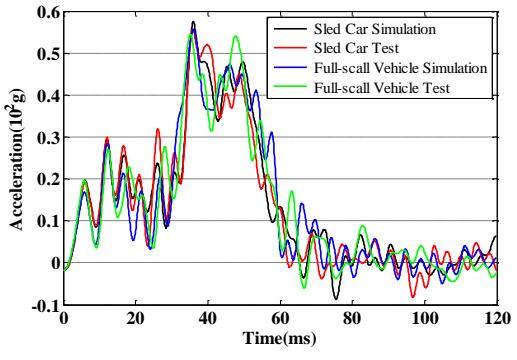


Figure 5: Acceleration history on the left sill of B-pillar

2. Finite element modeling of FLB-TRB

The deformation of the FLB has a mixed axial and bending mode under frontal impact. Compared with bending mode, the axial deformation will be a more appropriate mode for energy absorption and stability. According to the performance requirements, the FLB is divided into 4 different crush spaces (shown in Figure 6) in this study, where space A and space B are expected to generate a relatively uniform and progressive axial collapse, space C is defined by the dimensions of the engine compartment and space D expects high bending stiffness to resist bending deformation. Among these crush spaces, the spaces A, B and C belong to the crush zone, which are used to absorb kinetic energy, while the space D belongs to the transition zone, whose main aim is to transfer impact load.

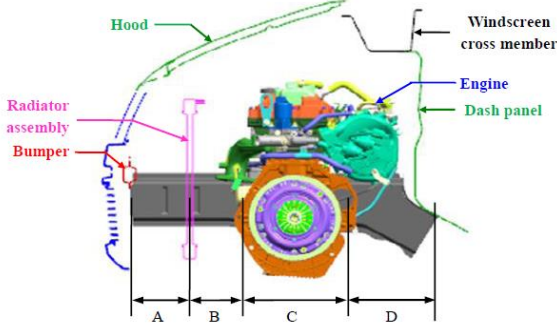


Figure 6: Crush spaces for front end structure

This work focuses on the lightweight design of FLB by combining the advantages of TRB manufacturing technology to maximize its weight reduction without compromising vehicle crashworthiness performances. Figure 7 show the schematic diagram of the whole manufacturing process of FLB-TRB, whose thickness customized can continuously vary along the rolling direction by adjusting the roll gap. The different roll spacing will produce different strain hardening, which directly results in different material properties. As a result, the variability of thicknesses and material properties in different local zones has to be considered in the numerical simulation of FLB-TRB. In order to address the issue, effective plastic stress-strain field should be constructed firstly. Then FE model of the FLB-TRB is modeled using 8-nodes thick shell elements (T-shell in LS-DYNA) [11].

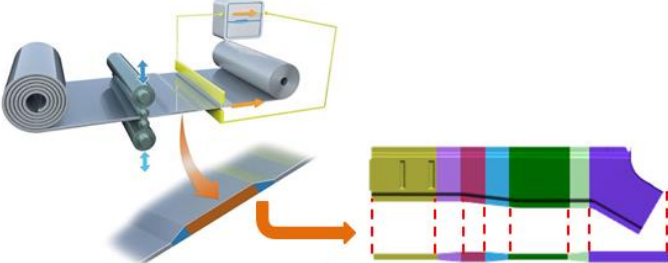


Figure 7: The schematic diagram of manufacturing process for FLB-TRB.

2.1 Material constitutive model for TRB

The material of FLB-TRB is HSLA340. Up to today, there is not material constitutive model for TRB available. In order to establish a relationship of strain vs. stress for the HSLA340 material of TRB, four specimens with thickness of 1.00, 1.17, 1.56 and 1.95mm are cut along the initial rolling direction to conduct uniaxial tensile tests on an INSTRON-5581 electronic universal testing machine. The effective stress-effective strain curves derived from test results are given in Figure 8. From which, it is easily found that the material properties of HSLA340 has a significant difference among the different thicknesses. Due to the expensive cost and time consuming of experimental tests, it is impractical to obtain the material characteristics of any thickness by experimental method. To address the issue, the piecewise linear interpolation method is used to interpolated the material performance of thickness from 1.0mm to 2.0mm.

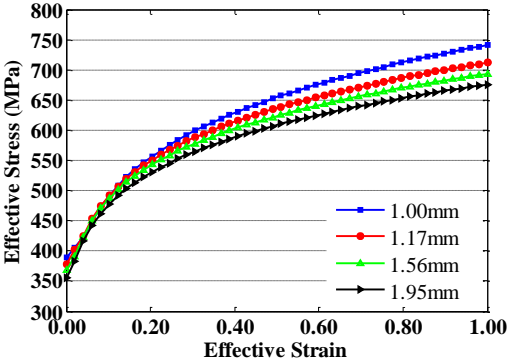


Figure 8: Effective stress-effective strain curves of HSLA340

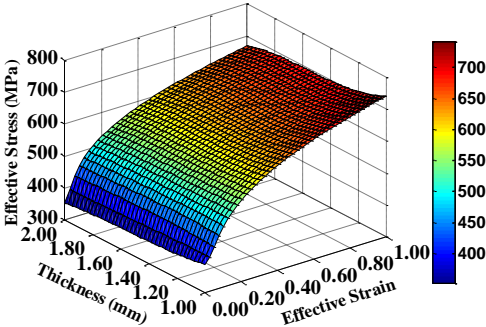


Figure 9: Effective stress-strain field of TRBs made of HSLA340

2.2 Finite element modeling of FLB-TRB

Figure 10(a) depicts the geometry model of the inner of TRB front longitudinal beam (TRB FLB-inner). To model the variable thickness of TRB, the 8-nodes thick shell element (T-shell in LS-DYNA) ^[11] was adopted. In which, the element of the constant thickness zone (CTZ) which has uniform mechanical property is organized into the same component, while the thickness transition zone (TTZ) needs to be divided into several components due to it has the non-uniform mechanical property, shown in Figure 10(b). The number of the components is decided by the modelling accuracy. In generally, the more the number of components are, the higher the modelling accuracy is. The material model used in the finite element modeling is piecewise linear plasticity material law (Mat 24 in LS-DYNA). The material performance of every component is calculated according to its thickness from Figure 9. The “automatic single surface” and “automatic surface to surface” contact are used in this model.

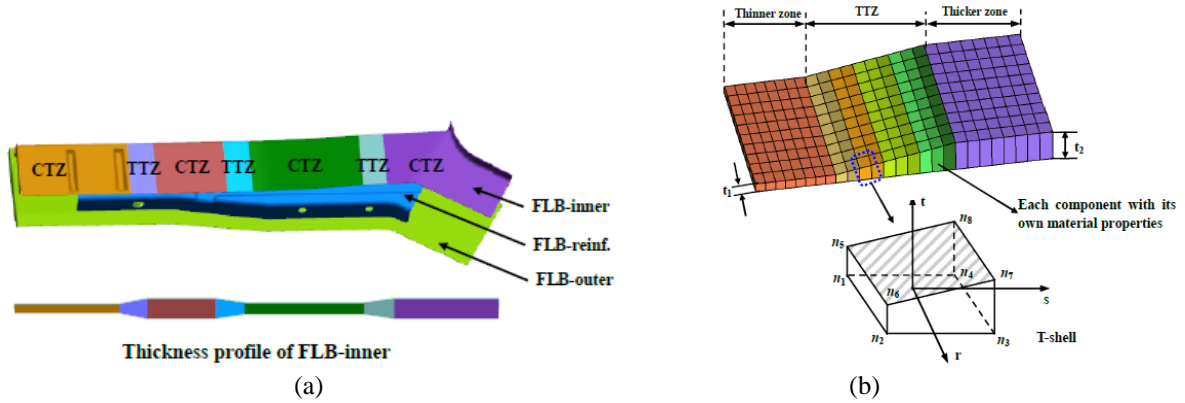


Figure 10: (a) Geometry model of TRB FLB-inner; and (b) FE model of TRB

3. Lightweight design of FLB-TRB under crashworthiness

Though the FLB-TRB has excellent potential of lightweight and crashworthiness, it is by no mean to obtain the optimal thickness distribution of FLB-TRB. Herein, structural optimization method was used to design the FLB-TRB. In the optimization progress, first, the conventional uniform thickness FLB panel is replaced with the TRB. Second, optimal Latin hypercube sampling (OLHS) ^[12] technique is used to generate sampling points and the objective and constraints function values are calculated using commercial software LS-DYNA. Following this the ϵ -SVR technique ^[13] is used to construct the surrogate models for the highly nonlinear impact responses. Finally, the Artificial Bee Colony (ABC) algorithm ^[14] is used to minimize the weight of TRB FLB-inner under the constraint of crashworthiness. The whole optimization procedure is shown in Figure 11.

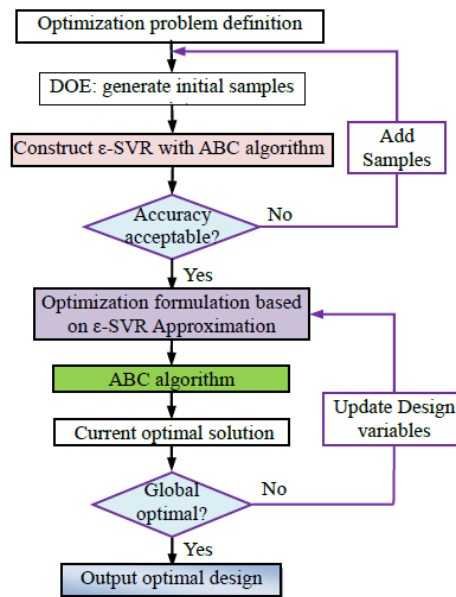


Figure 11: Flowchart of optimization process

3.1 Design responses and variables

In general, the crashworthiness of FLB can be evaluated by peak acceleration, energy absorption (FLB_EA), dash panel intrusion and FLB dynamic intrusion (Left and Right) [15, 16]. Hence, they are chosen as crashworthiness indicators of the simplified frontal impact model, represented by $A(x)$, $E(x)$, $S_1(x)$, $S_2(x)$ and $S_3(x)$, respectively. In addition, the weight of the TRB FLB-inner is regarded as the objective function, denoted by $M(x)$. The following three kinds of parameters are chosen as design variables: (a) thicknesses of constant thickness zone (CTZ), (b) length of thickness transition zone (TTZ) and (c) position of TTZ. Figure 12 shows the initial geometry parameters of the TRB FLB-inner with four different thickness segments. The design variables and their ranges are shown in Table 1.

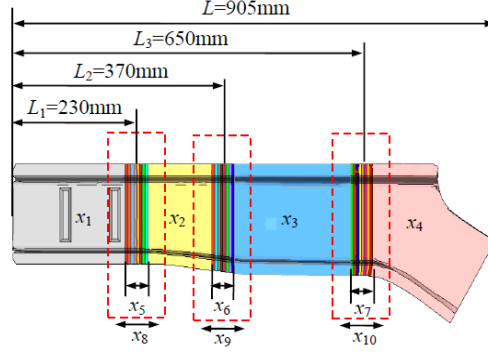


Figure 12: Geometry parameters of TRB FLB-inner

Table 1 Table 1 Geometry parameters of FLB-inner for dynamic impact (Unit: mm)

Variable	Description	Lower Bound	Upper Bound	Baseline Design
x_1	Thickness of CTZ	1.0	2.0	1.6
x_2	Thickness of CTZ	1.0	2.0	1.6
x_3	Thickness of CTZ	1.0	2.0	1.6
x_4	Thickness of CTZ	1.0	2.0	1.6
x_5	Length of TTZ	$Max(40, 100*(x_2-x_1))$	120.0	40.0
x_6	Length of TTZ	$Max(40, 100*(x_3-x_2))$	120.0	40.0
x_7	Length of TTZ	$Max(40, 100*(x_4-x_3))$	120.0	40.0
x_8	Position of TTZ	150.0	260.0	230.0
x_9	Position of TTZ	330.0	410.0	370.0
x_{10}	Position of TTZ	570.0	690.0	650.0

3.2 Optimization mathematical model

According to the description mentioned above, the optimization mathematical model can be written as:

$$\begin{cases} \min & M(\mathbf{x}) \\ \text{s.t.} & A(\mathbf{x}) \leq 57 \text{ g} \\ & E(\mathbf{x}) \geq 63000 \text{ J} \\ & S_1(\mathbf{x}) \leq 120 \text{ mm} \\ & S_2(\mathbf{x}) \geq 210 \text{ mm} \\ & S_3(\mathbf{x}) \geq 210 \text{ mm} \\ & \mathbf{x}^L \leq \mathbf{x} \leq \mathbf{x}^U, \quad \mathbf{x} = (x_1, x_2, x_3, x_4, x_5, x_6, x_7, x_8, x_9, x_{10})^T \end{cases} \quad (1)$$

where the constraint values are the responses of baseline design.

3.3 Optimization process

To establish high accuracy surrogates, OLHS technique is adopted to generate 300 sampling points and the output responses are calculated using commercial software LS-DYNA. Then, the ε support vector regression (ε -SVR) technique is used to construct the surrogate models for $M(x)$, $A(x)$, $E(x)$, $S_1(x)$, $S_2(x)$ and $S_3(x)$, respectively. The error measures applied for evaluating the model fitness, the squared correlation coefficient R_{CV-5}^2 and the root mean square error $RMSE_{CV-5}$ are calculated as follows:

$$R_{CV-5}^2 = \frac{1}{5} \sum_{j=1}^5 \left(1 - \frac{\sum_{i=1}^l (y_i - \hat{y}_i)^2}{\sum_{i=1}^l (y_i - \bar{y}_i)^2} \right) \quad (2)$$

$$RMSE_{CV-5} = \frac{1}{5} \sum_{j=1}^5 \sqrt{\frac{1}{l} \sum_{i=1}^l (y_i - \hat{y}_i)^2} \quad (3)$$

where l is the number of data points at each validation set, y_i is the observed response value, \hat{y}_i is the predicted value and \bar{y} is the mean value of y_i , respectively.

Table 2 lists the optimal parameters and the error results of the ε -SVRs. From which, it is easily found that the surrogates have a very high accuracy and can be used to the following design optimization.

Table 2 Optimal parameters and error results of ε -SVRs

Responses	C	ε	σ	R_{CV-5}^2	$RMSE_{CV-5}$
$M(x)$	23.4581	0.0986	2.2529	0.9929	0.0213
$A(x)$	0.6422	0.1961	1.5969	0.9688	0.0477
$E(x)$	34.7902	0.2438	1.4322	0.9728	0.0331
$S_1(x)$	1.5631	0.1331	1.9379	0.9810	0.0504
$S_2(x)$	2.9360	0.0436	3.3871	0.9631	0.0556
$S_3(x)$	18.1769	0.2322	1.4674	0.9867	0.0494

3.4 Optimization results and discussion

To obtain the optimal thickness profiles of FLB-inner without compromising vehicle crashworthiness, the ABC algorithm is used to solve the mathematical model. The iterative process of $M(x)$ is shown in Figure 13. From the Figure 13, it is easily found that the optimization progress was converges after 35 iterations. The optimal results are listed in Table 3 and the corresponding thickness profile of the TRB FLB-inner is shown in Figure 14.

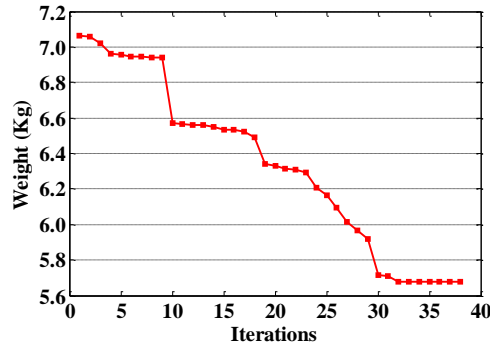


Figure 13: Iterative process of the weight of TRB FLB-inner

Table 3 Optimal results

Description	x_1	x_2	x_3	x_4	x_5	x_6	x_7	x_8	x_9	x_{10}
Baseline	1.60	1.60	1.60	1.60	40.0	40.0	40.0	230.0	370.0	650.0
Optimum	1.15	1.64	1.00	1.73	75.6	70.5	58.3	242.6	391.7	643.5

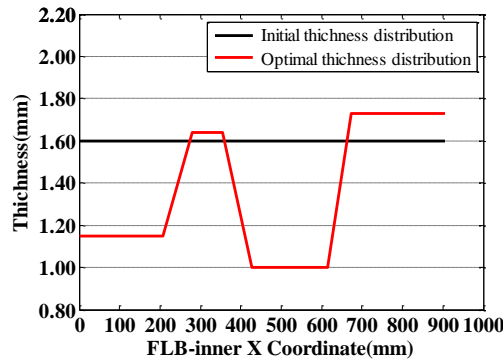


Figure 14: Thickness profile of TRB FLB-inner

Table 4 Improvements of vehicle performance for lightweight design optimization

Description	Baseline design	Optimal design	Improvement (%)
$M(x)$	6.77	5.68	-16.10%
$A(x)$	57.47	54.83	-4.59%
$E(x)$	61527.10	65846.79	7.02%
$S_1(x)$	136.24	106.81	-14.47%
$S_2(x)$	197.15	230.39	16.86%
$S_3(x)$	190.66	225.69	17.54%

Noted: $\text{Improvement} = \frac{\text{Optimal design} - \text{Baseline design}}{\text{Baseline design}} \times 100\%$

The Improvements of crashworthiness of TRB FLB-inner with respect to baseline design are listed in Table 4. Figure 15 compares the deformation patterns of the FLB before and after optimization. From which, it is easily found that the deformation patterns of the FLB can be greatly improved through the redistribution of thickness of the TRB FLB-inner. Figure 16 depicts the numerical results of crush pulses for the baseline and optimal design. In the baseline design, the space “B” of the front longitudinal beam buckled sideways and the space “D” happened sharp bending deformation, which greatly decrease the resistance load of the FLB. In the optimal design, the space “A” and space “B” occurred relatively uniform and progressive axial collapse and the previous sharp bending deformation disappeared in the space “D”, which leads to the reduction of peak acceleration. It is clearly shown from Table 4, Figure 15 and Figure 16 that optimal thickness distribution of the TRB FLB-inner can not only largely reduce its weight but also enhance vehicle crashworthiness.

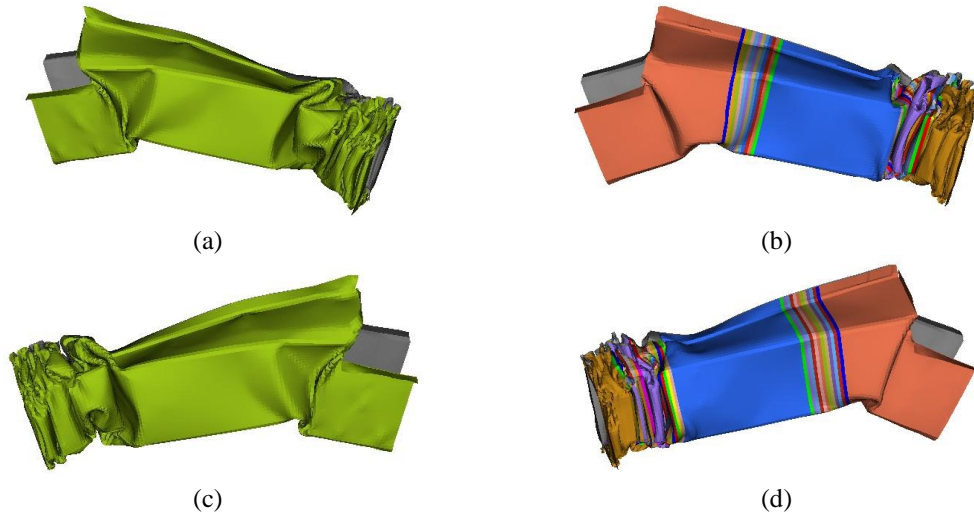


Figure 15 Comparison of the numerical result before and after optimization: (a) Left FLB of baseline design; (b) Left FLB of optimal design; (c) Right FLB of baseline design; and (d) Right FLB of optimal design

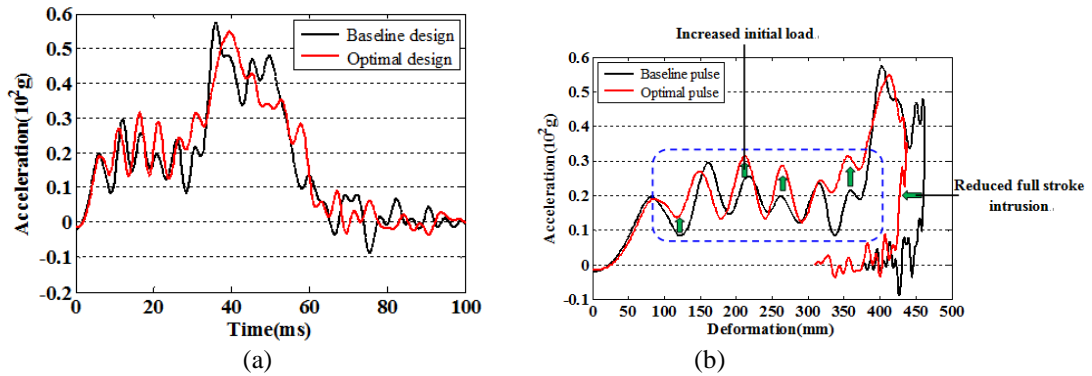


Figure 16 Comparison of crash pulses before and after optimization

4. Conclusions

In this work, the lightweight design of FLB-inner with TRB concept has been successfully performed under 100% frontal impact load case. The optimal solution shows that the weight of the FLB-inner can be reduced by 16.10%, while the crashworthiness is improved compared with the baseline design. It is clearly shown that the TRB technique has great potential to realize lightweight.

Acknowledgments

This work was supported from The National Natural Science Foundation of China (11202072, 61232014), The Doctoral Fund of Ministry of Education of China (20120161120005), National Natural Science Foundation of China (Grant No. 11202074), The Open Fund Program of the State Key Laboratory of Vehicle Lightweight Design, P. R. China (20130303), The Hunan Provincial Science Foundation of China (13JJ4036) and the Program of the Methodology Study on Designing Automotive Parts with Variable Thickness Blanks (QYT-KT-2013-003).

References

- [1] G.Y. Li, F.X. Xu, X.D. Huang and G.Y. Sun, Topology Optimization of an Automotive Tailor-Welded Blank Door, *Journal of Mechanical design*, 137(5), 055001 (May 01, 2015) (8 pages)
- [2] F. Pan, P. Zhu and Y. Zhang, Metamodel-based lightweight design of B-pillar with TWB structure via support vector regression, *Computers and Structures*, 88(1-2):36-44, 2010
- [3] Y.L. Shi, P. Zhu, L.B. Shen and Z.Q. Lin, Lightweight design of automotive front side rails with TWB concept, *Thin-Walled Structures*, 45(7):8-14, 2007
- [4] A. Meyer, B. Wietbrock and G. Hirt, Increasing of the drawing depth using tailor rolled blanks-Numerical and experimental analysis, *International Journal of Machine Tools & Manufacture*, 48, 522-531, 2008
- [5] S.J. Jeon, M.Y. Lee and B.M. Kim, Development of Automotive Door Inner Panel using AA 5J32 Tailor Rolled Blank, *Transactions of Materials Processing*, 20 (7): 512-517, 2011
- [6] G.Y. Sun, F.X. Xu, G.Y. Li and Q. Li, Crashing analysis and multiobjective optimization for thin-walled structures with functionally graded thickness, *International Journal of Impact Engineering*, 64, 62-67, 2014
- [7] G.Y. Li, F.X. Xu, G.Y. Sun and Q. Li, A comparative study on thin-walled structures with functionally graded thickness (FGT) and tapered tubes withstanding oblique impact loading, *International Journal of Impact Engineering*, 77, 68-83, 2015
- [8] G.Y. Sun, X. Tian, J. Fang, F. Xu, G. Li and X. Huang, Dynamical bending analysis and optimization design for functionally graded thickness (FGT) tube, *International Journal of Impact Engineering*, 78, 128-137, 2015
- [9] C.H. Chuang, R.J. Yang, G. Li, K. Mallela and P. Pothuraju, Multidisciplinary design optimization on vehicle tailor rolled blank design, *Structural and Multidisciplinary Optimization*, 35(6):551-560, 2008
- [10] G.X. Gu, G.Y. Sun, G.Y. Li, L.C. Mao and Q. Li, A Comparative study on multiobjective reliable and robust optimization for crashworthiness design of vehicle structure, *Structural and Multidisciplinary Optimization*, 48:669-684, 2013
- [11] J. Halquist, *LS-DYNA keyword user's manual version 971*. Livermore Software Technology Corporation, Livermore, CA, 2007
- [12] V.C.P. Chen, K.L. Tsui, R.R. Barton and M. Meckesheimer, A review on design, modeling and applications of computer experiments, *IIE Transactions*, 38(4): 273-291, 2006
- [13] V. Vapnik, *The nature of statistical learning theor*, Springer, Berlin, 1995
- [14] D. Karaboga and B. Basturk, A powerful and efficient algorithm for numerical function optimization: artificial bee colony (ABC) algorithm, *Journal of Global Optimization*, 39(3): 459-471, 2007
- [15] P. Zhu, Y. Zhang and G.L. Chen, Metamodel-Based Lightweight Design of Automotive Front Body Structure Using Robust Optimization, Proceedings of the Institution of Mechanical Engineers, Part D, *Journal of Automobile Engineering*, 223(9):1133-1147, 2009
- [16] F. Pan and P. Zhu, Lightweight design of vehicle front end structure: Contributions of multiple surrogates, *International Journal of Vehicle Design*, 57(2-3): 124-147, 2011